IEEE Access
Multidisciplinary ⋮ Rapid Review ⋮ Open Access Journal

Received January 20, 2022, accepted February 14, 2022, date of publication February 21, 2022, date of current version March 21, 2022.

Digital Object Identifier 10.1109/ACCESS.2022.3153108

Brain Tumor and Glioma Grade Classification Using Gaussian Convolutional Neural Network

MUHAMMAD RIZWAN[1], (Member, IEEE), AYSHA SHABBIR[1], ABDUL REHMAN JAVED[2], (Member, IEEE), MARYAM SHABBIR[3], THAR BAKER[4], (Senior Member, IEEE), AND DHIYA AL-JUMEILY OBE[5], (Senior Member, IEEE)

[1]Department of Computer Science, Kinnaird College for Women, Lahore 54000, Pakistan
[2]Department of Cyber Security, Air University, Islamabad 44000, Pakistan
[3]School of Professional Advancement, University of Management and Technology, Lahore 54770, Pakistan
[4]Department of Computer Science, College of Computing and Informatics, University of Sharjah, Sharjah, UAE
[5]School of Computer Science and Mathematics, Liverpool John Moores University, Liverpool L3 5UX, U.K.

Corresponding author: Dhiya Al-Jumeily Obe (d.aljumeily@ljmu.ac.uk)

ABSTRACT Understanding brain diseases such as categorizing Brain-Tumor (BT) is critical to assess the tumors and facilitate the patient with proper cure as per their categorizations. Numerous imaging schemes exist for BT detection, such as Magnetic Resonance Imaging (MRI), generally utilized because of the better quality of images and the reality of depending on non-ionizing radiation. This paper proposes an approach to detect distinctive BT types using Gaussian Convolutional Neural Network (GCNN) on two datasets. One of the datasets is used to classify tumors into pituitary, glioma, and meningioma. The other one separates the three grades of glioma, i.e., Grade-two, Grade-three, and Grade-four. These datasets have '233' and '73' victims with a total of '3064' and '516' images on T1-weighted complexity improved pictures for the first and second datasets, separately. The proposed approach achieves an accuracy of 99.8% and 97.14% for the two datasets. The experimental results highlight the efficiency of the proposed approach for BT multi-class categorization.

INDEX TERMS Deep learning, brain tumor classification, Gaussian convolutional neural network.

I. INTRODUCTION

An uncontrolled and unnatural brain cell's development is known as BT [1]. The human brain is volume-restricted and a rigid body; therefore, a human capacity may be influenced by an unforeseen development; in addition, this might proliferate into other body organs and result in life-threatening conditions [2]–[4].

As per the worldwide (tumor growth) report, provided by the World Health Organization (WHO), BT lies under 2% of human cancer; extreme dismalness, complexities, and comorbidities also exist. Tumor-oriented research in the UK estimated approximately around 52, 250, succumbing to intracranial, Central-Nervous-System (CNS), and brain tumors in the United Kingdom. Existing studies report that around 30% of BTs are benign tumors. BTs classification can be classified based on the severity and type, such as malignant and benign tumors. Such categorization is based on the tumor's source. Mainly, tumors can be defined as the tumor whose initial source is the brain, whereas the secondary tumor is the tumor whose initial source is some other part of the body, and later proliferated towards the brain, and the vast majority of the secondary tumors are dangerous [5]. Radiological images are one of the most widely recognized non-intrusive sources. Due to avoiding any ionizing radiation, MRI is most popular these days. Additionally, by using enhanced-contrast features or utilizing different imaging features, MRI can acquire images, and it possesses super-resolution power for soft tissues [6]. Various imaging procedures can be utilized to recognize and characterize BT [7].

The most common BTs are Glioma-tumors that start in the brain's Glial Cells (GCL). Gliomas incorporate 30% of CNS, BTs, and 80% of malignant BTs. WHO classified Glioma-tumors into four types, i.e., type-one to type-four. Grade-one BTs are benevolent and possess very identical

The associate editor coordinating the review of this manuscript and approving it for publication was Wentao Fan.

surfaces to the GCLs. Grade-two BTs are marginally texture-wise distinct. Grade-three BT is dangerous (possess strange tissue appearance), whereas Grade-four BTs are the super extreme phase of tissue irregularities and gliomas, which can be observed through the eye [4].

Meningioma-Tumors (MTs) develop tranquility (among all BTs). It develops (inside the brain) on the spinal rope, and the cerebrum covers the layer. The vast majority of MTs are less severe/benign. Nonetheless, pituitary-organs oriented tumor is known as Pituitary-Tumors (PTs). In the human body, PTs direct and control hormones. It may proliferate towards bones and can be dangerous/malignant. At the same time, it may be less dangerous/benign. Difficulties of PTs comprise of vision loss or inadequacy of perpetual hormones [4], [8].

Due to the above-referenced knowledge, early BT's discovery and detection transform into an essential errand and likewise assist (to protect the patient's life) in choosing the most accessible curing approach. Besides, the categorization stage might be a confounding and monotonous task (for radiologists and doctors) in some sensitive cases. These cases need specialists to deal with tumor localization, contrast the tissues of tumor and neighboring locales, filter the picture if essential, make it all more straightforward for human vision, lastly, regardless of whether this is BT other than its grade and sort. We propose a more efficient deep learning based approach using a Gaussian filter for pre-processing (for noise filtering and smoothing the input images). It is time-consuming, and we require Computer-Aided Design (CAD) based approach (without human intercession) for the earliest identification of BTs.

The significant contributions of this research are listed below:

- We propose customized Gaussian Convolutional Neural Network (GCNN) for brain tumor type (i.e., pituitary, glioma, and meningioma) and glioma's grade (i.e., grade-1, grade-two, grade-three, and grade-four) classification.
- We apply and analyze various filters for pre-processing (for noise filtering and smoothing the input images) of BT images to improve the classification.
- We present a comparative analysis with state-of-the-art and standard machine learning algorithms.
- Results show that CNNA with Gaussian filter outperforms other common image pre-processing filters and provides better BT classification.

The rest of the paper is organized as follows. Related work is presented in Section II. The proposed work is presented in Section III. Experimental analysis is presented in Section IV. Result and discussion is given in Section V, and conclusion is provided in Section VI.

II. RELATED WORK

Authors in [9] presented a brain-inspired hybrid system for the symbiotic intelligence of humanity. They pretend theoretical foundations, intelligence, knowledge-based system, and cognitive analysis towards developing next-generation cognitive systems. Using the patterns and without any outside instruction, particular tasks can be performed (with statistical inferences and algorithms) in Machine Learning (ML) can be done by cognitive computing [10]. AI algorithms have been generally developed in the clinical imaging field as a part of machine learning [4], [11]–[15]. Being a constituent of AI, ML schemes are now immensely utilized in bio-informatics. This has two primary classes, unsupervised and supervised. In the supervised learning strategies, the input to output mapping is done using different mapping algorithms to predict unforeseen samples. The objective is to learn inalienable correlations inside the data for training purposes, utilizing ML schemes such as K-Nearest Neighbors Algorithm (KNNA), Support Vector Machine Algorithm (SVMA), and Artificial Neural Network Algorithm (ANNA) [16]–[18].

Conversely, only input parameters are used in unsupervised-learning algorithms, such as in Self Organization-Map Algorithm (SOMA) and fuzzy-c-mean algorithm. The feature extraction of training images is crucial, i.e., statistical parameters (for learning purposes), texture, and grayscale, and this might demand tumor segmentation before extracting the features. We can define them as handcrafted features, where a specialist is demanded with the proficiency to categorize the required features. Besides, in the case of big data size, it is inclined to errors and time-consuming. DLA develops AI-oriented models and frameworks that depend on information portrayals and progressive component learning. For feature extraction, DLA uses various layers of processing with nonlinearity. As we dive deep into the network, the yield of each successive layer is the contribution of the following one. Additionally, it assists in data abstraction. CNNA is a class of DLA and ordinarily utilized in visual imaging analysis also, intended to require little pre-processing [19], [20].

CNNA is motivated by natural procedures in the brain [21] and used to deal with distinct forms of data. The earlier utilization of the DLA with a comparison of its present application (presented a century ago) when Lecun presented a DLA "lenet" (in 1998), and it was utilized in the applications, where it was required to perform document's recognition. Numerous years later, it became considerably more mainstream directly (in the wake of utilizing DLA to perform the image classification by using a framework known as 'AlexNet' (AN)) [22]. During this session, AN showed extraordinary results with other utilized algorithms.

BT characterization has been performed utilizing numerous AI procedures, and imaging modalities [6]. Feature-learning and provision of robust accuracy-rate are the primary favorable points of CNNA (instead of conventional vanilla neural systems and machine learning which might be accomplished by expanding the training data), and in this way, it prompts a more robust and more precise model. For feature extraction, convolutional filters are utilized in the CNNA protocol. Heavily complex features (structural and spatial data) are extracted as we dive deeper into the network.

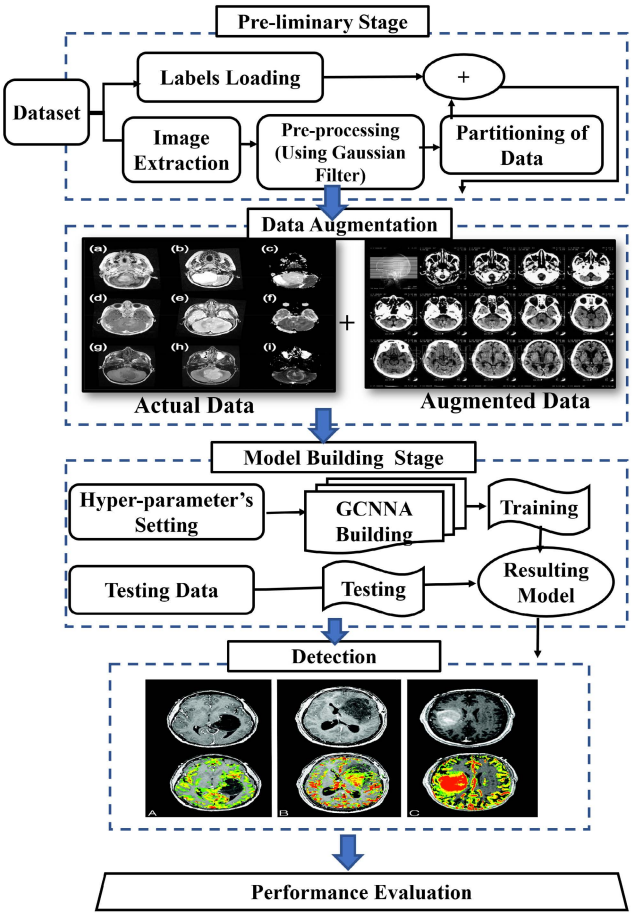

FIGURE 1. Proposed work diagram.

With the input patterns, feature-extraction occurs through convolution of small-filters, followed by the most distinctive feature selection, and prepares the network for classification purposes.

For multi-categorization, the accuracy rate of 85% and 88% for binary-categorization is acquired. Authors in [23] presented a technique for the classification of 80 BT abnormal and normal CT images utilizing 'Discrete Wavelet Transform' approach (DWTA) for feature-extraction, 'Principal Component Analysis' Approach (PCAA) for feature-reduction, and afterward for image-oriented classification is performed using ANN and KNNA with a precision of 97% and 98% separately. For feature extraction, three schemes are utilized, i.e., Bag-of-Words and intensity-histogram.

Comprising two joined resolutions, another model for the BT image classification (i.e., dependent on CNNA and Genetic-Algorithms (GA-CNNA)) is presented by Anaraki *et al.* [24]. Posteriorly, a capsule network (CapsNetK) is presented by Afshar *et al.* [25], that coordinates both the brain image's MRI and the coarse tumor, limited to the BT classification. Through this study, 90.89% of precision was acquired. A precision rate of 90.9% has been achieved (for the first analysis) to classify three glioma grades. The subsequent contextual investigation acquired a 94.2% precision rate for pituitary, meningioma, and glioma tumor classification.

III. PROPOSED WORK

A customized CNNA is proposed to categorize various grades and types of BT. The system's design is enhanced utilizing diverse configurations to acquire the most suitable framework. The proposed work's diagram is depicted in Fig. 1.

From the raw files of the dataset, the loading and extraction of labels and images are done. After splitting the training, validation, and testing data, the data is preprocessed and augmented. By setting the optimization algorithm, regularization approach, and hyper-parameters structure, the structure of the proposed work is presented. At last, the execution and training framework of the network is provided. Algorithm 1 provides the processing of the proposed work [26].

This paragraph elucidates the working of the Algorithm 1. First, the images are acquired by the system (as input), and the respective type of brain tumor is classified as output. At the initial stage, while performing the preprocessing, the color-space (of images) is transformed to convert them to grayscale images; the input images are cropped to smoothen the images and remove noise, the Gaussian filter is convolved over the input images. Next, after categorizing the labeled and unlabeled dataset, the model is tunned (through the training phase) in a hit and trial approach (where the hyper-parameters are selected). Backpropagation is performed if the error rate exceeds the threshold value and readjusted weights. Lastly, the true positives, true negatives, false positives, and false negatives are acquired from the results.

A. PRE-PROCESSING

Pre-processing is carried out before passing the CT scans into the algorithm. To boost the system for simpler computations and to exhibit superior performance in less time, the first step is to reduce the dimensionality of the actual images from $512 \times 512 \times 1$ to $128 \times 128 \times 1$-pixels. At that point, data is rearranged before parting them to prepare the unsorted data. After splitting the data, three parts are generated: training, validation, and test data (with every instance having a labeled target value). 35% of data is selected for validation and testing purposes and 65% for training purposes.

After that, to increment the model's robustness and to abstain from overfitting, data augmentation is done so that the framework can recognize it as new data. The images are augmented with a salt-noise/grayscale distortion (the geometric-augmentation). The actual three thousand sixty-one images are augmented (by the multiple of five) through the augmentation approach. Finally, for type classification, the last dataset of fifteen thousand three hundred seventeen images is acquired, and for grade classification, five hundred thirteen image-based datasets are utilized.

B. ARCHITECTURE OF GCNN

Fig. 2 presents the structure of GCNN. For pre-processing of input images, a Gaussian filter is applied (after having

Algorithm 1 Brain Tumor Classification Using GCNN.

Input: data ← Input Images of BT
Output: Type of BT (Pituitary,Glioma, and Meningioma) and Gioma Grade (Grade-II, Grade-III, Grade-IV)

```
Pre-processing ← image crop, rotate, flip, induce noise, transform the color-space, GF application.
D_label ← Data_Labeled
D_Ulabel ← Data_UnLabeled
M_learn ← Model_Learning
D_train ← Data_Training
P_train ← Phase_training
M_tune ← Model_tunning
M_train ← Model_training
T_iterations ← Total_Iterations
T_Value ← Threshold_Value
Utilize D_train to acquire M_tune
D_synthetic ← {}
while a_j, b_i∈P_train do
    Synthesization of s samples {a_i, b_i}p^m
    M_train
    D_synthetic ← D_syntheticU{a_i, b_i}p^m
end while
M_tune ← tunning(parameters, D_label, M_learn)
for i = 1:T_iterations do
    Forward_Propagation
    Predicted_label = Classify: (target_label, loss_rate)
      ← M_tune(D_Ulabel)
    for instance of D_Ulabel
    if Predicted_label == target_label) then
        # True_Positive, True_Negative
    else
        # False_Positive, False_Negative
        Evaluation of Loss
        if error_rate > T_value then
            Back_propagation
            Updation of Weights
        end if
    end while
end for
Evaluation of Accuracy
return Detected_Output
```

a comparative analysis among multiple imaging filters). After that, sixteen layers are incorporated, from pre-processing augmented images to the input layer, later downsampling (through Pooling, Normalization, Rectified-Linear-Unit (ReLU), and convolution), feature-selection, and convolution operation are performed. By using the dropout layer, overfitting is avoided. Later for the output prediction fully connected layer and softmax layer are utilized, and for the classification of predicted-class, a classification layer is added. The whole layered structure of CNNA is given in Fig. 2.

Four convolutional layers are utilized in the suggested work. Each layer's depiction is as follows; the input layer is utilized for data normalization and input (i.e., images of BT) size confirmation. By the movement of filters on the input BT images and by input's and weight's dot-product computation (where each filter of MXN size and there are K filters), a 2D convolution is applied. By following the horizontal and vertical steps, the sliding of filters/kernels is done on the input images, known as a stride. Before sliding the kernel, the actual image's padding is done. As feature-identifiers, these filters are utilized. The low-level highlights (blobs, lines, and edges) are classified by initial layers filters, whereas the advanced layers are utilized for complex feature detection.

An example is shown in Fig. 3, where after dot-product and filter-sliding a 3×3 dimensional input is generated (when on an image of 3×3 size, a 3×3 sized filter is applied). The values of the parameters are; for first, second convolutional-layer P = [2, 2, 2, 2], [2,2,2,2], and [0,0,0,0]; S = [1, 1]; M × N = 2×2, 3×3, and 10×10; and K = 128,128,and 64. To decrease the training time as compare to other activation-functions; ReLU is used here (that is non-saturated in nature) and it is following each convolutional-layer. Fig. 3 shows the convolution operation.

The below-provided condition portrays as a function of y i.e. the ReLU activation-function. Here if y is +ve then results are equal to the inputs and for other cases it would be 0 (see Eq. (1)).

$$f(y) = max(0, y) \tag{1}$$

The input's normalization is done by adjusting and scaling associated activation operations. At that point, the input layer is standardized by a cross-channel normalization layer. With a specific sized window (which is discretionarily picked as five), (channel-wise) a reaction standardization/normalization layer is used. The normalization layer is utilized in network training and backpropagation.

To acquire spatial invariance, small rectangles (of 2×2 size) are generated from a single image, and this kind of down-sampling is done through the max-pooling layer. For the 2×2 matrix, over the image, they are moved, and from the four values, the only max value is considered. Reduction in the network's computation is made by reducing the number of attributes, which is carried out with the help of the pooling layer. The pooling layer is utilized to decrease the parameter's quantity and subsequently the network calculations. Fig. 4 depicts an example of max-pooling. By using the dropout layer, the overfitting reduction is made. For the first and second dropout-layer, the highly appropriate dropout values are ten% and twenty%, respectively. Lastly, Classification (CLF), Softmax (SFT), and FC Layers are used. These are ordered as FC, SFT, and CLF, respectively. A few nodes/enactments are dropped out arbitrarily in this layer, which fundamentally helps in the training-stage acceleration.

The previous one is utilized to associate one layer's neurons to each other's neurons (preceding and following). At that point, a standardized exponential function is utilized, where the SFT layer follows the FC layer. To squash all the predicted categorizations somewhere in the range

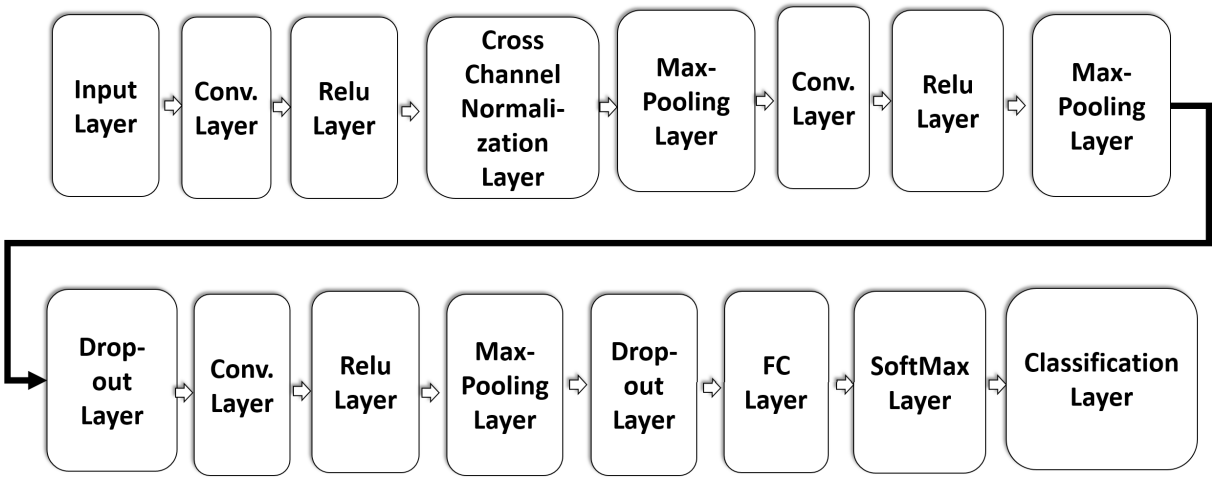

FIGURE 2. GCNN framework.

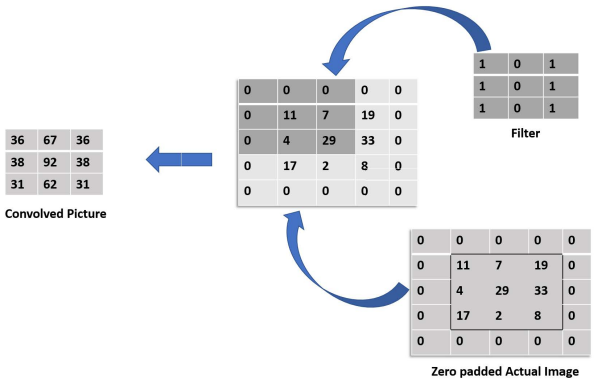

FIGURE 3. Convolutional layer example (input: 3 × 3, zero padding: 1, kernel size: 3 × 3, Stride: 1, output: 3 × 3).

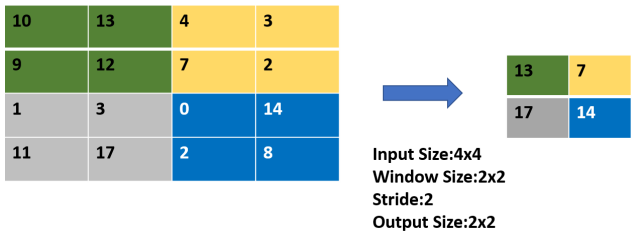

FIGURE 4. Max-pooling pperation (input: 3 × 3, zero-padding: 1, kernel size: 3 × 3, Stride: 1, output: 3 × 3).

of 0-1, the SFT layer is utilized, and the absolute entirety of these qualities is equivalent to one that is a hundred%. The yield of this layer can be determined as follows:(see Eq. (2))

$$z(a)_k = -(e_k^a)/(\sum_{(}^{l} l = 1)e_k^a) \tag{2}$$

The kth-class likelihood is computed using function z(a) over l distinct output classes (whose complete summation is equivalent to one). A cross-entropy-oriented classification layer is added at last for each input BT image prediction and estimation of prediction error rate. Eq. (3, shows the error-rate estimation. Here from the SFT-layer, r (y) is the vector for classified output, and q is the vector for target-label is the vector for target-labels (see Eq. (3)). The next section elaborates on the optimized algorithm and the regularization approach.

$$I(q, r) = -\sum_{y}(q(y) * log(q(y))) \tag{3}$$

Regularization is meant to fit the function to avoid overfitting while training the model. Numerous methods are utilized during training and pre-processing stages to abstain from overfitting. One of these approaches is augmenting the data, where the actual pictures are augmented through color & geometric distortion (to prevent overfitting). At that point, diverse frameworks of the network are being tried to deflect the complex nature of the network. Additionally, to stochastically evacuate the weights of hidden units, dropout layers are being utilized [27]. The below equation Eq. (4) shows the decay of weight and penalty addition to the cost-operation using L2 regularization.

$$cost = cost(loss) + \lambda \sum_{(}^{l} j = 1)X_j^2 \tag{4}$$

The hyper-parameter is represented by λ (regularization attribute), and the respective weight(s) is represented by x for $j = 1, \ldots,$ l. To avoid overfitting and ensure the stability of the model, the validation and training process is monitored time by time (before the completion of entire epochs), and all this is done through an early-stopping approach. Through convergence (by making little moves to the direction of negative-gradient) and approaching the global minimum, optimization is done (where loss-rate is minimized and the network parameters are updated) [28]. For the proposed work, momentum-oriented stochastic-gradient-descent is founded as the optimal optimizer. FIGURE 5 shows the flowchart of the system's working.

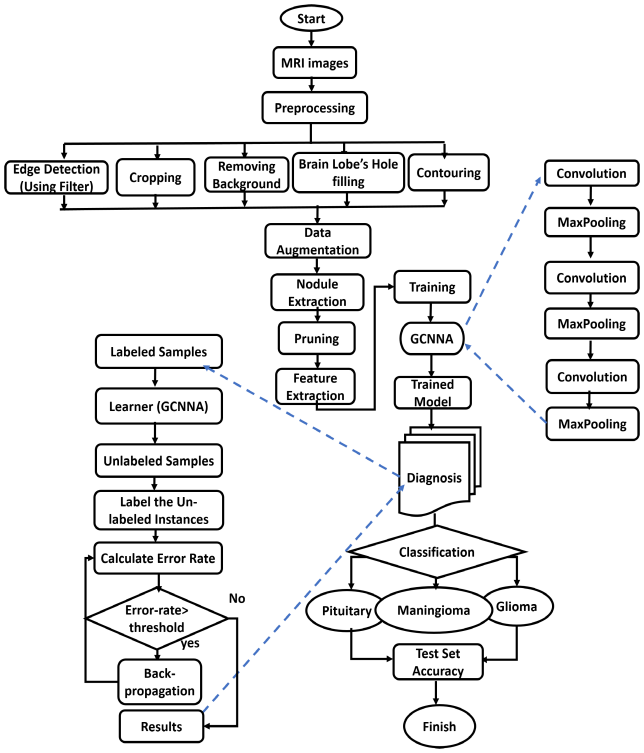

FIGURE 5. Flow chart of the proposed work.

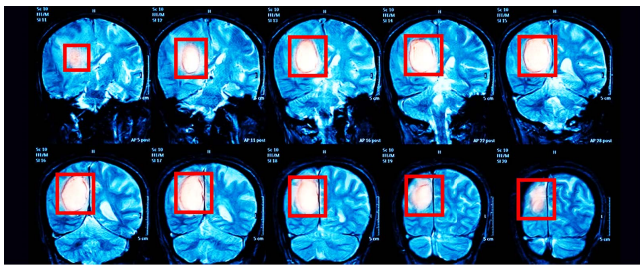

FIGURE 6. BT classification.

IV. EXPERIMENTS AND OUTCOMES

The two diverse datasets used in this work are obtained from General Hospital and Nanfang Hospital, Medical University of Tianjin, China from 2005-2010.[12] This dataset incorporates ''T1-weighted complexity improved pictures''. Three kinds of BTs (i.e., pituitary, glioma, and meningioma) are procured from 232 patients [29]. BTs can be various fits from the perspective of size, location, and shape as indicated by the respective grade and type as shown in Fig. 6. The dataset incorporates three distinct perspectives: sagittal, coronal, and axial, as appeared in Fig.6.

The second dataset is retrieved from a public repository, ''The Cancer Imaging Archive (TCIA).''[3] The repository contains MRI multi-sequence image scans of distinct ages, races, maladies, and evaluations of 129 patients with Molecular Brain Neoplasia Data (REMBRANDT) [30]. We select BT images on T1-weighted complexity, incorporating various glioma grades (Grade-two, Grade-three, and Grade-four) as shown in Fig. 7. The explanation of the two datasets is provided in Table 1 and Table 2.

We apply image shifting before applying CNNA as a pre-handling stage. This is critical to identify the BT image's edges. Therefore, it is required to smooth, sharp, and remove the noise of the BT's input pictures. The comparative view of various basic imaging filters is depicted to perform their performance analysis (see Fig. 8). After this experiment, the

[1]https://www.med.upenn.edu/sbia/brats2018/data.html
[2]https://figshare.com/articles/dataset/brain_tumor_dataset/1512427
[3]https://www.cancerimagingarchive.net/

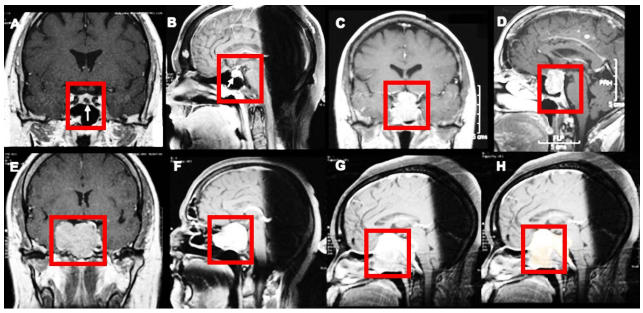

FIGURE 7. BT classification-II.

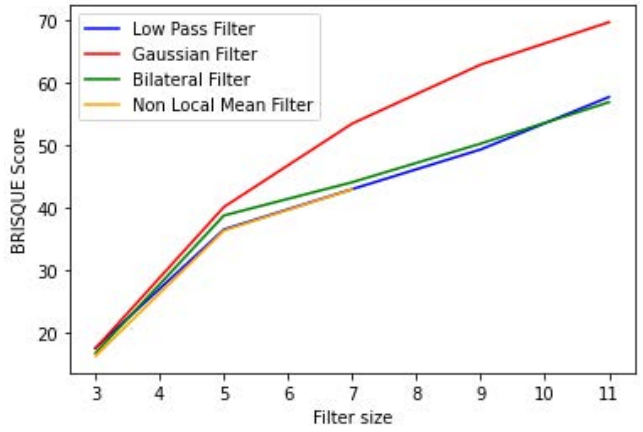

FIGURE 8. Comparison of imaging filters.

TABLE 1. First dataset description.

Category	Slices	Patients
Pituitary-tumor	929	59
Glioma-Tumor	1425	90
Meningioma-tumor	707	81
	3061	230

TABLE 2. Second dataset description.

Category	Patients	Slices
Grade-two	204	32
Grade-three	128	18
Grade-four	181	20
	513	70

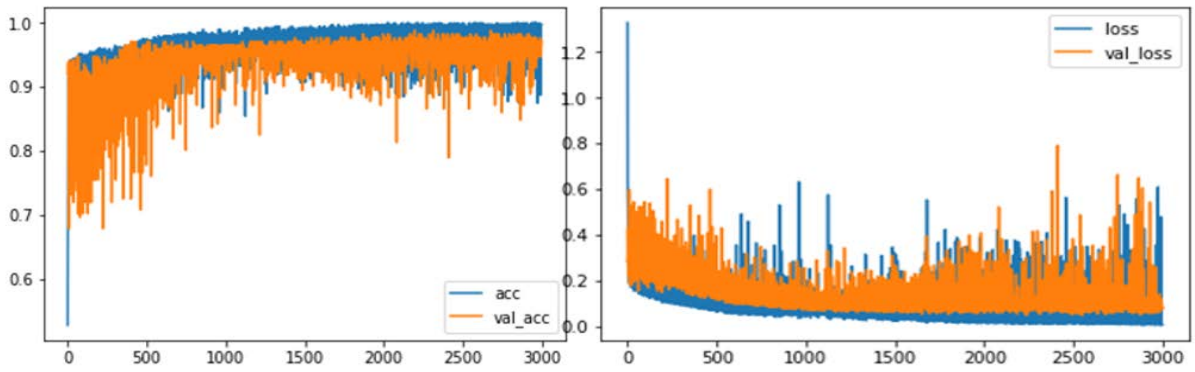

FIGURE 9. Validation-accuracy and validation-loss for experiment-I: (a) validation-accuracy on left side, and (b) validation-loss right side.

best consequences of Gaussian-Filter (GF) are acquired, and for preprocessing of BT's images, GF is applied (that is why it is known as Gaussian Convolutional Neural Network-GCNN). Next, the filter size is elucidated by the horizontal axis, and the BRISQUE is represented by the vertical axis (after applying the particular GF, it addresses the image's quality). FIGURE 9, case-I shows both the exact progress and error rate during the proposed work's approval stage. Almost 100% precision is accomplished as depicted in Fig. 9(a). It shows the results after total iterations of 5000^{th}. After the 8515^{th} iteration, the accuracy level achieved is almost 100%. Lastly, the best overall precision obtained during the test stage is 96.13%. The loss-graph in small-batches is shown in Fig.9(b). The bend begins to drop pointedly, yet a minor uncertainty shows up because of utilizing a diminutive group size of 32 pictures. These variances tend to vanish after the total iterations of 6400, and the loss curve is nearly 0.

For case-II, both the validation and loss are shown in Fig. 10. It can be seen that the training accuracy of almost 100% is accomplished at around 1000 iterations. Consequently, the best accuracy of 98.7% is acquired during the test stage as shown in Fig. 10(a). Fig. 10(b) presents the loss-graph (for small-batches). The loss-graph nearly hits zero, and after 100 iterations, this incline is in general stopped.

The performance matrix is presented in Table 3. We use Accuracy, Specificity, Sensitivity, and Precision. Here, the quantity of positive anticipated class is known as True-Positive-Case (TPC), which are positive cases. The quantity of negative anticipated classes is regarded as True-Negative-Case (TNC), which are also really negative cases. The quantity of negative anticipated class while that is positive-case, also called as error type-two-error.

The proposed approach achieved 97.54% accuracy for meningioma, glioma 95.81%, and pituitary-categorization resulting in a 96.89% accuracy rate. A 100% accuracy is achieved in the categorization of glioma-Grade-two, 95% for glioma-Grade-three, and 100% for glioma-Grade-four.

A. HYPER-PARAMETERS AND EMPIRICAL ARCHITECTURES

We tune parameters of the distinct architectures (engaged with the procedure of selection). The distinctive tested parameters are given in Table 4 to get the presented final structure, representing the best performance level.

B. PLATFORM AND TIME COMPLEXITY

The proposed structure of GCNN is prepared using Python, MATLAB 2019b, 32GB RAM, Intel-i5-7700HQ CPU (2.5 GHz). Training for '10417' pictures is '299' minutes in experiment-I and experiment-II. For '350' pictures, it is recorded as 2.5 minutes. Thus, the normal execution time for the test is 8.4 and 9.7 milliseconds per picture for the first and second datasets, separately.

V. DISCUSSION

By applying the GCNN framework to the MRIM, this manuscript comprises a methodology for BTs characterization and glioma tumor grades classification. Before acquiring the final model, customization of various parameters of the GCNN model is done. Without underfitting and overfitting, GCNN training is a very critical one, as this may require months or weeks (for a dataset) to acquire the desired consequences. Table 5, we list the results from past literary works (utilized for similar BT types with different layers, hyper-parameters, and architecture). Comparatively, the proposed structure gives the best prediction outcomes contrasted with other related literature studies, which show the dependability of the proposed framework. In addition, the proposed GCNN is a division-free technique (when the BT's images are loaded) to acquire the related classification results.

Despite utilizing pathological pictures to prepare the system, not many favorable outcomes have been acquired by combining two classifiers. Conversely, feature-engineering is utilized to remove highlights and afterward decrease their measurements to utilize them in another phase for detection and categorization. In different researches, the authors have utilized a Genetic Algorithm (GA) to demonstrate the

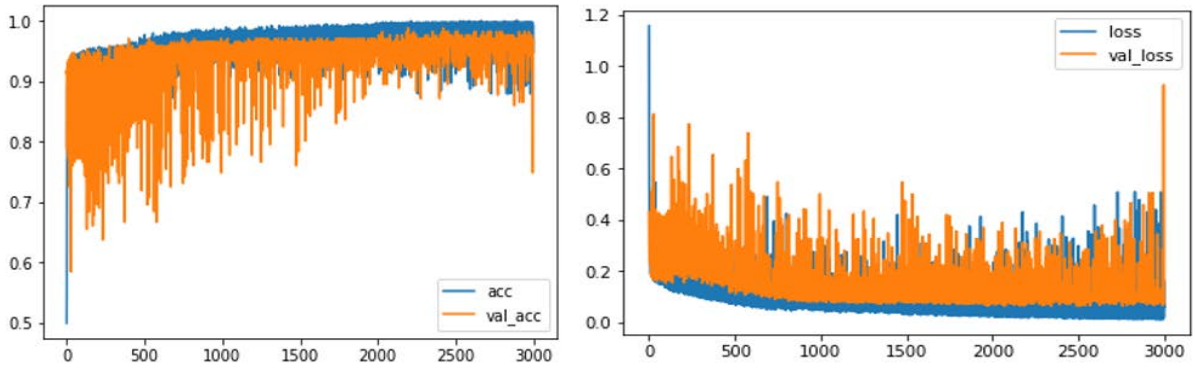

FIGURE 10. Validation-accuracy and validation-loss for experiment-II: (a) validation-accuracy on left side, and (b) validation-loss on right side.

TABLE 3. Results of the proposed approach.

Method	Type	True-Positive	True-Negative	False-Positive	False-Negative	Total	Precision	Accuracy
For first dataset (brats2018) [31]	Pituitary-tumor	679	1565	33	47	698	0.967	97.81
	Glioma-tumor	1025	1194	32	60	1070	0.983	96.72
	Meningioma	516	1743	21	23	548	0.962	98.92
For second dataset (TCIA) [32]	II-grade	32	45	1	1	33	0.99	99
	III-grade	18	58	1	2	22	0.99	96
	IV-grade	25	51	2	1	99	0.97	99

TABLE 4. Specifications of GCNN.

Parameter	Value
ReLU & Conv.layers	1-4
Normalization layers	1-3
Drop-out layer	1-3
Epochs	200, 400, 500, 600, 800, 1000, 3000
FC layers	1-3
Conv. filters	16, 24, 40, 128, 512
Kernel size	2-11(prime values)
Pooling	avg. & max. pooling
Size of window	2-5
Optimiser	RMS prop, Adam, SGD
Size of mini-batch	2^0 to 2^7
Dropout-rate	0.5, 0.25, 0.2, 0.15. 0.1
Learning-rate (initially)	0.0001, 0.001, 0.01
Drop-factor in learning	$0.1 - 0.3$

TABLE 5. Comparative analysis with existing studies. Key: multi-classification- MC, binary-classification-BC, genetic algorithm CNNA-GA-CNNA.

Ref.	Experiment-I	Experiment-II	Type	Approach
[33]	91.43%	-	MC	CNNA
[25]	90.89%	-	MC	CNNA
[24]	90.89%	-	MC	GA-CNNA
[34]	71%	-	MC	CNNA
[34]	96%	-	BC	CNNA
Proposed	99.8%	97.14%	MC	GCNN

system's engineering. However, GA did not present the ideal forecast results. In [33], the authors have utilized just two convolutional layers with 64-kernels for each. Additionally, they have utilized four dropout layers which are moderately high for the introduced network.

The authors in [25] have utilized coarse tumor limits as an extra contribution to help the system in providing better outcomes. However, the upcoming stages need more procedures to confine the tumor before preparing a CNNA. Even though we have accomplished a reasonable classification rate, the proposed framework in this experimentation needs to be tried for more enormous scope datasets that incorporate various other parameters to build its portability convenience and expand it in other clinical applications later on. Also, the framework's structure cannot be reused to detect the modest number of pictures as it is one of the limitations of DLA, yet rather than that, the framework can be fine-tuned in the wake of preparing on an extensive dataset (after having a small dataset).

VI. CONCLUSION

This paper presented a CAD approach for detecting and categorizing BT's radiological images into three kinds (pituitary-tumor, glioma-tumor, and meningioma-tumor). We also classified glioma-tumor into various categories (Grade-two, Grade-three, and Grade-four) utilizing the GCNN approach(i.e., our proposed work). In this paper, first preprocessing is done using a Gaussian imaging filter, and later sixteen layers based network is generated. These layers are ordered like input layer convolutional layers (along with activation functions). CLF Layer (for output class categorization) follows the SFT and FC layers, following the dropout layer (for overfitting prevention). Data augmentation proved favorable to depict effective outcomes, even though the dataset is generally not huge (because of the assortment of imaging views). The presented work has accomplished (utilizing two datasets) the most noteworthy accuracy rate of 97.14% and 99.8% through this research.

REFERENCES

[1] M. I. Razzak, M. Imran, and G. Xu, "Efficient brain tumor segmentation with multiscale two-pathway-group conventional neural networks," *IEEE J. Biomed. Health Informat.*, vol. 23, no. 5, pp. 1911–1919, Sep. 2019.

[2] B. Lei, P. Yang, Y. Zhuo, F. Zhou, D. Ni, S. Chen, X. Xiao, and T. Wang, "Neuroimaging retrieval via adaptive ensemble manifold learning for brain disease diagnosis," *IEEE J. Biomed. Health Informat.*, vol. 23, no. 4, pp. 1661–1673, Jul. 2019.

[3] A. Mikhno, F. Zanderigo, R. T. Ogden, J. J. Mann, E. D. Angelini, A. F. Laine, and R. V. Parsey, "Toward noninvasive quantification of brain radioligand binding by combining electronic health records and dynamic PET imaging data," *IEEE J. Biomed. Health Informat.*, vol. 19, no. 4, pp. 1271–1282, Jul. 2015.

[4] N. Abiwinanda, M. Hanif, S. T. Hesaputra, A. Handayani, and T. R. Mengko, "Brain tumor classification using convolutional neural network," in *World Congress on Medical Physics and Biomedical Engineering*. Bhopal, India: Springer, 2019, pp. 183–189.

[5] A. Tiwari, S. Srivastava, and M. Pant, "Brain tumor segmentation and classification from magnetic resonance images: Review of selected methods from 2014 to 2019," *Pattern Recognit. Lett.*, vol. 131, pp. 244–260, Mar. 2020.

[6] G. Litjens, T. Kooi, B. E. Bejnordi, A. A. A. Setio, F. Ciompi, M. Ghafoorian, J. A. Van Der Laak, B. Van Ginneken, and C. I. Sánchez, "A survey on deep learning in medical image analysis," *Med. Image Anal.*, vol. 42, pp. 60–88, Dec. 2017.

[7] S. Kadry, Y. Nam, H. T. Rauf, V. Rajinikanth, and I. A. Lawal, "Automated detection of brain abnormality using deep-learning-scheme: A study," in *Proc. 7th Int. Conf. Bio Signals, Images, Instrum. (ICBSII)*, Mar. 2021, pp. 1–5.

[8] T. Meraj, A. Hassan, S. Zahoor, H. T. Rauf, M. I. Lali, L. Ali, and S. A. C. Bukhari, "Lungs nodule detection using semantic segmentation and classification with optimal features," *Neural Comput. Appl.*, vol. 33, no. 17, pp. 10737–10750, 2019.

[9] Y. Wang, W. Kinsner, S. Kwong, H. Leung, J. Lu, M. H. Smith, L. Trajkovic, E. Tunstel, K. N. Plataniotis, and G. G. Yen, "Brain-inspired systems: A transdisciplinary exploration on cognitive cybernetics, humanity, and systems science toward autonomous artificial intelligence," *IEEE Syst., Man, Cybern. Mag.*, vol. 6, no. 1, pp. 6–13, Jan. 2020.

[10] M. Chen, F. Herrera, and K. Hwang, "Cognitive computing: Architecture, technologies and intelligent applications," *IEEE Access*, vol. 6, pp. 19774–19783, 2018.

[11] T. Hossain, F. Shishir, and M. Ashraf, "Brain tumor detection using CNN," *Turkish J. Comput. Math. Educ.*, vol. 12, no. 11, pp. 4597–4603, 2021.

[12] P. R. Krishnaveni and G. N. Kishore, "Image based group classifier for brain tumor detection using machine learning technique," *Traitement Signal*, vol. 37, no. 5, pp. 865–871, Nov. 2020.

[13] J. Amin, M. Sharif, M. Raza, T. Saba, and M. A. Anjum, "Brain tumor detection using statistical and machine learning method," *Comput. Methods Programs Biomed.*, vol. 177, pp. 69–79, Aug. 2019.

[14] K. Muhammad, S. Khan, J. D. Ser, and V. H. C. D. Albuquerque, "Deep learning for multigrade brain tumor classification in smart healthcare systems: A prospective survey," *IEEE Trans. Neural Netw. Learn. Syst.*, vol. 32, no. 2, pp. 507–522, Feb. 2021.

[15] E. Irmak, "Multi-classification of brain tumor mri images using deep convolutional neural network with fully optimized framework," *Iranian J. Sci. Technol., Trans. Electr. Eng.*, vol. 4, pp. 1–22, Oct. 2021.

[16] P. R. Kshirsagar, A. N. Rakhonde, and P. Chippalkatti, "MRI image based brain tumor detection using machine learning," *Test Eng. Manage.*, vol. 4, pp. 3672–3680, Jan. 2020.

[17] S. Pereira, A. Pinto, V. Alves, and C. A. Silva, "Brain tumor segmentation using convolutional neural networks in MRI images," *IEEE Trans. Med. Imag.*, vol. 35, no. 5, pp. 1240–1251, May 2016.

[18] C. Ma, G. Luo, and K. Wang, "Concatenated and connected random forests with multiscale patch driven active contour model for automated brain tumor segmentation of MR images," *IEEE Trans. Med. Imag.*, vol. 37, no. 8, pp. 1943–1954, Aug. 2018.

[19] C.-W. Zhang, M.-Y. Yang, H.-J. Zeng, and J.-P. Wen, "Pedestrian detection based on improved LeNet-5 convolutional neural network," *J. Algorithms Comput. Technol.*, vol. 13, Sep. 2019, Art. no. 1748302619873601.

[20] D. Zhang, G. Huang, Q. Zhang, J. Han, J. Han, and Y. Yu, "Cross-modality deep feature learning for brain tumor segmentation," *Pattern Recognit.*, vol. 110, Mar. 2021, Art. no. 107562.

[21] P. M. Shakeel, T. E. El Tobely, H. Al-Feel, G. Manogaran, and S. Baskar, "Neural network based brain tumor detection using wireless infrared imaging sensor," *IEEE Access*, vol. 7, pp. 5577–5588, 2019.

[22] A. Krizhevsky, I. Sutskever, and G. E. Hinton, "ImageNet classification with deep convolutional neural networks," in *Proc. Adv. Neural Inf. Process. Syst. (NIPS)*, Dec. 2012, pp. 1097–1105.

[23] A. Kutlu, "A novel method for classifying liver and brain tumors using convolutional neural networks, discrete wavelet transform and long short-term memory networks," *Sensors*, vol. 19, no. 9, p. 1992, Apr. 2019.

[24] A. K. Anaraki, M. Ayati, and F. Kazemi, "Magnetic resonance imaging-based brain tumor grades classification and grading via convolutional neural networks and genetic algorithms," *Biocybernetics Biomed. Eng.*, vol. 39, no. 1, pp. 63–74, Jan./Mar. 2019.

[25] P. Afshar, K. N. Plataniotis, and A. Mohammadi, "Capsule networks for brain tumor classification based on MRI images and coarse tumor boundaries," in *Proc. IEEE Int. Conf. Acoust., Speech Signal Process. (ICASSP)*, May 2019, pp. 1368–1372.

[26] V. Rajinikanth, S. Kadry, R. Damasevicius, D. Taniar, and H. T. Rauf, "Machine-learning-scheme to detect choroidal-neovascularization in retinal OCT image," in *Proc. 7th Int. Conf. Bio Signals, Images, Instrum. (ICBSII)*, Mar. 2021, pp. 1–5.

[27] C. Szegedy, W. Liu, Y. Jia, P. Sermanet, S. Reed, D. Anguelov, D. Erhan, V. Vanhoucke, and A. Rabinovich, "Going deeper with convolutions," in *Proc. IEEE Conf. Comput. Vis. pattern Recognit.*, Mar. 2015, pp. 1–9.

[28] L. Bottou, "Large-scale machine learning with stochastic gradient descent," in *Compstat*. Paris, France: Springer, 2010, pp. 177–186.

[29] J. Cheng, "Brain tumor dataset," Tech. Rep., Apr. 2017.

[30] L. Scarpace, A. Flanders, R. Jain, T. Mikkelsen, and D. W. Andrews, "Data from rembrandt. the cancer imaging archive," Tech. Rep., 2015.

[31] J. Cheng, W. Huang, S. Cao, R. Yang, W. Yang, Z. Yun, Z. Wang, and Q. Feng, "Enhanced performance of brain tumor classification via tumor region augmentation and partition," *PLoS ONE*, vol. 10, no. 10, Oct. 2015, Art. no. e0140381.

[32] K. Clark, B. Vendt, K. Smith, J. Freymann, and J. Kirby, "The cancer imaging archive (TCIA): Maintaining and operating a public information repository," *J. Digit. Imag.*, vol. 26, no. 6, pp. 1045–1057, Dec. 2013.

[33] J. S. Paul, A. J. Plassard, B. A. Landman, and D. Fabbri, "Deep learning for brain tumor classification," *Proc. SPIE Biomed. Appl. Mol., Struct., Funct. Imag.*, vol. 10137, Dec. 2017, Art. no. 1013710.

[34] M. G. Ertosun and D. L. Rubin, "Automated grading of gliomas using deep learning in digital pathology images: A modular approach with ensemble of convolutional neural networks," in *Proc. AMIA Annu. Symp.*, 2015, p. 1899.

MUHAMMAD RIZWAN (Member, IEEE) received the M.Sc. degree from PUCIT, Lahore, Pakistan, in 2006, the M.S. degree from CIIT, Lahore, in 2012, and the Ph.D. degree from HUST, Wuhan, China, in 2017. In 2017, he joined as an Assistant Professor with the Department of Computer Science, Kinnaird College for Women, Lahore. He has authored or coauthored several peer-reviewed articles in professional journals and the proceedings of conferences. His research interests include the areas of machine learning algorithms, wireless sensor networks, mobile computing, self-organized networks, big data analytics, and the Internet of Things.

AYSHA SHABBIR is currently pursuing the M.S. degree with the Department of Computer Science, Kinnaird College for Woman, Lahore, Pakistan. Her research interests include machine learning, wireless sensor networks, mobile computing, and security issues in mobile cloud computing.

ABDUL REHMAN JAVED (Member, IEEE) received the master's degree in computer science from the National University of Computer and Emerging Sciences, Islamabad, Pakistan. He has worked at the National Cybercrimes and Forensics Laboratory, Air University, Islamabad, where he is a Lecturer with the Department of Cyber Security. He is a cybersecurity researcher and practitioner with industry and academic experience. He has reviewed over 150 scientific research articles for various well-known journals. He has authored over 50 peer-reviewed research articles and is supervising/co-supervising several graduate (B.S. and M.S.) students on topics related to health informatics, cybersecurity, mobile computing, and digital forensics. His current research interests include but are not limited to mobile and ubiquitous computing, data analysis, knowledge discovery, data mining, natural language processing, smart homes, and their applications in human activity analysis, human motion analysis, and e-health. He aims to contribute to interdisciplinary research of computer science and human-related disciplines. He is a member of ACM. He is a TPC Member of CID2021—Fourth International Workshop on Cybercrime Investigation and Digital Forensics and the 44th International Conference on Telecommunications and Signal Processing. He had served as a Moderator in the 1st IEEE International Conference on Cyber Warfare and Security (ICCWS).

MARYAM SHABBIR received the M.S. degree from the Department of Computer Science, Kinnaird College for Women, Lahore, Pakistan. Currently, she is a Lecturer with the School of Professional Advancement, University of Management and Technology, Lahore. She has authored or coauthored several peer-reviewed articles in professional journals and the proceedings of conferences. Her research interests include machine learning, wireless sensor networks, mobile computing, data analysis, knowledge discovery, data mining, natural language processing, and security issues.

THAR BAKER (Senior Member, IEEE) received the Ph.D. degree in autonomic cloud applications from Liverpool John Moores University (LJMU), U.K., in 2010 and became a Senior Fellow of the Higher Education Academy, in 2018. He was a Lecturer of computer science with the Department of Computing and Mathematics, Manchester Metropolitan University, U.K. He was a Reader of cloud engineering and the Head of the Applied Computing Research Group, Faculty of Engineering and Technology, LJMU. He is an Associate Professor with the Department of Computer Science, University of Sharjah (UoS), UAE. He has published numerous refereed research papers in his research areas. His research interests include parallel and distributed computing, algorithm design, green and sustainable computing, and energy-routing protocols.

DHIYA AL-JUMEILY OBE (Senior Member, IEEE) is a Professor of artificial intelligence and the President of the eSystems Engineering Society. He has extensive research interests covering a wide variety of interdisciplinary perspectives concerning the theory and practice of applied artificial intelligence in medicine, human biology, environment, intelligent community, and health care. He has published well over 300 peer-reviewed scientific international publications, 12 books, and 14 book chapters in multidisciplinary research areas, including machine learning, neural networks, signal prediction, telecommunication fraud detection, AI-based clinical decision-making, medical knowledge engineering, human–machine interaction, intelligent medical information systems, sensors and robotics, and wearable and intelligent devices and instruments. His current research interest includes decision support systems for self-management of health and medicine.